REFRIGERATION SCIENCE AND TECHNOLOGY
PROCEEDINGS

26th IIR International Congress of Refrigeration

Paris, France
August 21-25, 2023

Vol 4
Commissions: E1, E2

INSTITUT INTERNATIONAL DU FROID
INTERNATIONAL INSTITUTE OF REFRIGERATION

ISBN: 978-2-36215-058-6 ISSN: 0151-1637 Code: 2023-4

SCIENCE ET TECHNIQUE DU FROID
COMPTES RENDUS

26th International Congress of Refrigeration
August 21-25, 2023

Palais des Congrès de Paris
Paris Congress Center
2 place de la Porte Maillot
75017 Paris, France

Editor

Association Française du Froid (AFF)
French Association of Refrigeration

177 boulevard Malesherbes
75017 Paris, France
info@icr2023.org
https://www.icr2023.org

Publisher

Institut International du Froid (IIF)
International Institute of Refrigeration (IIR)
177 boulevard Malesherbes
75017 Paris, France

Scientific committee members

PRESIDENT
Jocelyn BONJOUR
Vice President of the IIR Science and Technology Council for the congress
Vice President commission B1

VICE-PRESIDENTS
Marc CLAUSSE
Rémi REVELLIN

MEMBERS
Gérald CAVALIER, *President of the IIR Science and Technology Council*
Ralf HERZOG, *President of Section A*
Ales SRNKA, *President of Commission A1*
Peng ZHANG, *President of Commission A2*
Eckhard A. GROLL, *President of Section B*
Yunho HWANG, *President of Commission B1*
Ji Hwan JEONG, *President of Commission B2*
Judith EVANS, *President of Section C*
Noboru MOTOMURA, *President of Commission C1*
Alain LE BAIL, *President of Commission C2*
Richard LAWTON, *President of Section D*
Kuniaki KAWAMURA, *President of Commission D1*
Silvia MINETTO, *President of Commission D2*
Renato LAZZARIN, *President of Section E*
Xianting LI, *President of Commission E1*
Alberto CORONAS, *President of Commission E2*

CONGRESS VICE PRESIDENTS
Dominique VALENTIAN, *Commission A1*
Philippe HAGYARD, *Commission A2*
Laurence FOURNAISON, *Commission B1*
Mohammed YOUBI-IDRISSI, *Commission B2*
Guillaume SAINT-LORANT, *Commission C1*
Alain LE BAIL, *Commission C2*
Nicolas PONDICQ CASOU, *Commission D1*
Thomas SUQUET, *Commission D2*
Eric DEVIN, *Commission E1*
Brice TREMEAC, *Commission E2*

COMMISSION E2 - HEAT PUMPS & ENERGY RECOVERY

DOI: 10.18462/iir.icr.2023.0077

Experimental results of a high-temperature heat pump prototype with R1336mzz(Z) for various production temperatures

Adrián MOTA-BABILONI*, Ángel BARRAGÁN-CERVERA, Cosmin Mihai UDROIU, Pau GIMÉNEZ-PRADES, Joaquín NAVARRO-ESBRÍ

ISTENER Research Group, Department of Mechanical Engineering and Construction, Universitat Jaume I
Castelló de la Plana, E-12071, Spain, istener@uji.es
*Corresponding author: mota@uji.es

ABSTRACT

Vapour compression heat pumps are the most promising technologies for decarbonisation in high-temperature processes. This paper presents experimental data of a high-temperature heat pump prototype designed for R-245fa when operating with R1336mzz(Z). Forty-five steady-state experiments were performed in a scroll compressor prototype with a liquid-to-suction heat exchanger at production temperatures between 102 °C and 158 °C (temperature difference of the secondary fluid between 8.5 K and 22 K) and waste heat temperatures between 80 °C and 118 °C (temperature difference of the secondary fluid between 12.6 K and 47.5 K). The heating capacity varied between 9.9 kW and 13.4 kW, and the coefficient of performance was between 2.0 and 4.8. Compared to previous experimental results using R-245fa, R-1336mzz(Z) results in higher COP under the same operating conditions. A medium-to-low carbon emission factor would make this solution more environmentally friendly than a natural gas boiler for small-scale heating production.

Keywords: HTHP, low GWP, COP, renewable heating, decarbonisation, waste heat

1. INTRODUCTION

High-temperature heat pumps (HTHP) are a technology that can recover waste heat and upgrade it to useful temperatures for other processes of the same industry. Among different sectors, Obrist et al. (2023) found that HTHPs are cost-efficient in the pulp and paper industry and the food and beverage industry and help reach policy goals regarding energy efficiency and CO_2e emission mitigation. Therefore, electrification of the heat supply with HTHP is also cost-efficient for reaching net-zero CO_2e emissions. Regarding industrial steam generation, the HTHP will keep getting attractive from a cost and emission perspective as the electricity grid will have a higher renewable energy share (Saini et al., 2023). Besides, compared to solar thermal collectors, the land requirement for HTHP is much smaller. They highlight that HTHP needs more developments for low-GWP refrigerants as a drawback. Jiang et al. (2022) conclusions agree with Saini et al. (2023) and ask for the development of green refrigerants with better characteristics and adaptability studies for drop-in replacements are the long-term prospects for refrigerants. Hydrofluoroolefins (HFOs) and Hydrochlorofluorolefins (HCFOs) have been developed to relieve the environmental impact (zero ozone depletion potential (ODP), low global warming potential (GWP) and shorter atmospheric lifetime), and natural refrigerants have been revived in research and application. Among different refrigerants, R-1336mzz(Z) is zero ODP, ultra-low GWP, and can be used at high temperatures compared to other refrigerants proposed for HTHPs. HFO-1336mzz(Z) breakdown in the trifluoroacetic acid (TFA) yield is expected to be about 0% to 4% (EFCTC, 2021).

After a literature review of the R-1336mzz(Z) molecule, Giménez-Prades et al. (2022) concluded that interest in R-1336mzz(Z) has been increasing in the last years, particularly as an HTHP working fluid. R-1336mzz(Z) thermophysical properties have been intensively researched, but only up to 80 °C and pressures 5 MPa. Moreover, R1336mzz(Z) is unsuitable as an R-245fa drop-in replacement due to the lower heating capacity than other alternatives, such as R-1233zd(E) or R-1224yd(Z). The most remarkable advantage of R-1336mzz(Z) is that it offers a relatively high critical temperature, 171 °C, suitable for several industrial processes.

Mateu-Royo et al. (2019) conducted a thermodynamic study of new low-GWP alternatives. R-1336mzz(Z) required a minimum superheat of 19.2 K. HFO-1336mzz(Z) improved COP by about 21% when using the LSHX compared to a basic configuration. HFO-1336mzz(Z) COP is comparable at variable heat production temperatures but requires higher compressor displacement for keeping R-245fa heating production. Arpagaus and Bertsch (2021) compared R-1224yd(Z), R-1233zd(E), R-1336mzz(Z), and R-245fa in a laboratory 10 kW HTHP with liquid-to-suction heat exchanger (LSHX) and variable-speed reciprocating. Up to heat sink temperatures of about 110 °C, R-1336mzz(Z) had a slightly lower COP due to the lower heating capacity and higher relative heat losses. The integration of the LSHX resulted in a significant COP increase, and the POE oil acid number after 100 operating hours in the HTHP revealed a low oil degradation.

HTHPs are a promising technology for industrial decarbonisation and provide renewable heating. The associated challenge to the HTHP technology is reducing the current technological development. This paper presents the experimental results of an HTHP prototype using the 4th generation synthetic refrigerant R-1336mzz(Z). The parameters analysed are compression ratio, mass flow rate, production temperature, heating capacity, and coefficient of performance. This experimental data can be used in further projects for developing models and predicting operational behaviour and energy performance.

2. MATERIALS AND METHODS

2.1. Experimental setup

The experimental setup comprises four closed-loop circuits to simulate the operation of HTHPs. The primary circuit simulates the operation of a vapour compression cycle (VCC) with a liquid-to-suction (intermediate) heat exchanger. Heat load is connected to an electrical boiler using thermal oil as heat transfer fluid (HTF). The heat sink circuit comprises two circuits: a closed loop circuit connected to a rooftop fan coil using water as an HTF and an intermediate circuit that uses thermal oil and can reach temperatures above 100 °C without the risk of boiling.

The complete experimental setup is displayed in Fig. 1. Selected pipelines and components are insulated to avoid heat losses to the ambient, which has been detrimental to the resulting system's energy performance in previous tests. The VCC contains a scroll compressor modified by the research group for operation as a high-temperature compressor/expander (admission volume of 121,1 cm^3 and 2900 rpm at 50 Hz), condenser and evaporator plate heat exchangers, and an electronic expansion valve. This circuit includes other necessary elements such as a subcooler, liquid-to-suction heat exchanger, bypass valves, and filter dryer. When selecting the elements, attention has been devoted to the maximum allowable temperature, pressure, and compatibility with refrigerants. The rest of the circuits contain an HTF pump with a frequency inverter and elements necessary for safe operation.

Refrigerant temperature (J-type thermocouple) and pressure (piezoelectric pressure transducer) are measured at the inlet and outlet of each main element of the VCC. Moreover, the mass flow rate using a Coriolis effect mass flowmeter and compressor power consumption from a digital wattmeter has also been measured. Inlet and outlet heat exchanger temperatures and volumetric flow rate (vortex) have been measured in the secondary circuits.

Operating conditions are controlled through PID in the electronic expansion valve, fan coil, and electric boiler (outlet evaporator temperature and pressure, heat sink temperature, and heat sink water temperature).

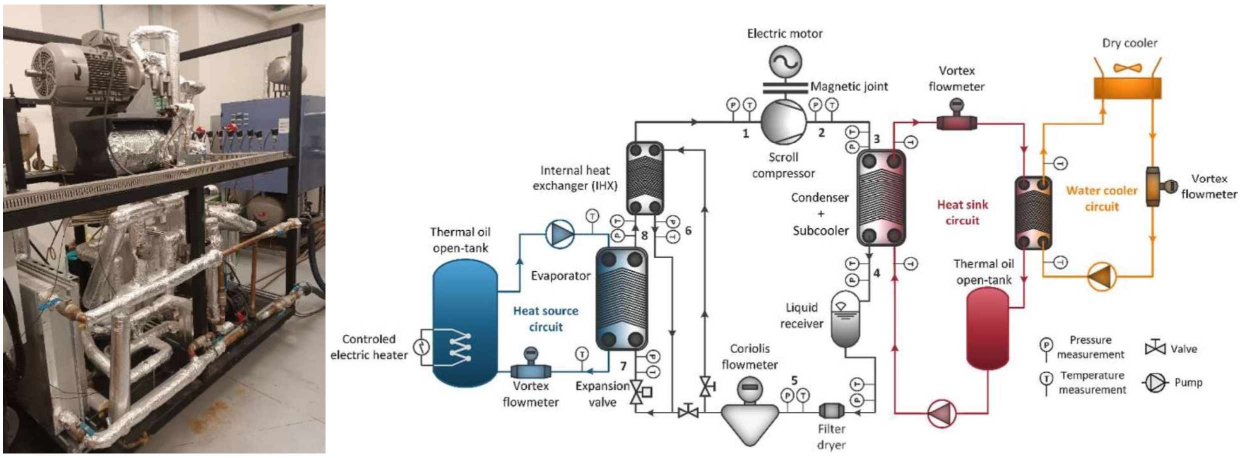

Figure 1: HTHP experimental setup

2.2. Experimental procedure

Operational and energy parameters shown in this article have been selected as follows. When the steady-state condition is reached, the operation is recorded for 20 minutes with a sampling period of 1 second when all essential circuit temperatures are identified as stable. The most representative 5 minutes conditions are selected with a maximum deviation for the heat sink, and the source temperatures were ±0.3 K and ±0.15 K. Then, the average parameters were determined, and the thermodynamic states of the refrigerant were determined using REFPROP v10.0 and steady-state experimental measurements.

Two refrigerants have been tested in this experimental setup, R-245fa and R-1336mzz(Z). The main properties of both refrigerants are shown in Table 1. Between the substitution of refrigerants, a compressor replacement has been performed. The first experimental tests with R-245fa used a modified scroll compressor, following know-how developed in organic Rankine cycle technology. In the following, R-1336mzz(Z) experimental tests included a commercial scroll compressor (7.5 kW and 22 $m^3\ h^{-1}$ at 50 Hz), in which a higher production temperature has been achieved.

Table 1: Main properties of R-1336mzz(Z) and R-245fa

Refrigerant	T_{crit}	P_{crit}	ρ_{dew} at 75 °C	NBP	M	ODP	GWP_{100}	Safety Class
	°C	*MPa*	*kg m^{-3}*	*°C*	*g mol^{-1}*	*R-11e*	*CO_2e*	
R-245fa	154.0	3.65	38.7	15.1	134.0	0	858	B1
R-1336mzz(Z)	171.4	2.90	24.1	33.4	164.1	0	2	A1

Production temperature refers to the condenser outlet considering the intermediate thermal oil closed loop circuit. This circuit simulates the maximum temperature delivered to an industrial process with renewable heating needs. The heat source circuit, connected to the evaporator, simulates the temperature at which an industrial process has exchanged heat and is cooled with the ambient (energy is lost). The frequency has been set to 40 Hz in the compressor because of limitations caused by the heat sink's nominal heating capacity.

2.3. Experimental tests

The final evaporation and condensation conditions for the high-temperature 40 Hz tests are shown in Figure 2. Condensation temperatures and evaporation temperatures (calculated using the average pressure at the inlet of the condenser and evaporator, respectively) varied between 119.7 °C and 152.6 °C, and 69.7 °Cand 85.2 °C, respectively. Therefore, the condensation temperature increased more than the evaporation temperature, resulting in a higher pressure ratio in the most critical conditions.

Total superheating and subcooling degree (considering suction and liquid lines and LSHX effects) also increased from 23.1 to 32.3 K and 22.3 and 29.8 K, respectively. Because pipes were adequately insulated, the superheating and subcooling were not affected by losses to the ambient (contrary to refrigeration systems, the superheating degree would decrease). A significant part of the superheating (57% to 70%) was caused by the LSHX (the rest occurred at the evaporator, 9.6 K to 10.2 K, controlled by the electronic expansion valve); therefore, a significant subcooling degree was caused on the other side of the LSHX (84% to 92% of the total subcooling degree). LSHX superheating and subcooling degree increased at higher condensation temperatures, and the same happens with the influence on the total superheating and subcooling degree. In the same way, LSHX thermal effectiveness also increased for higher condensation temperatures.

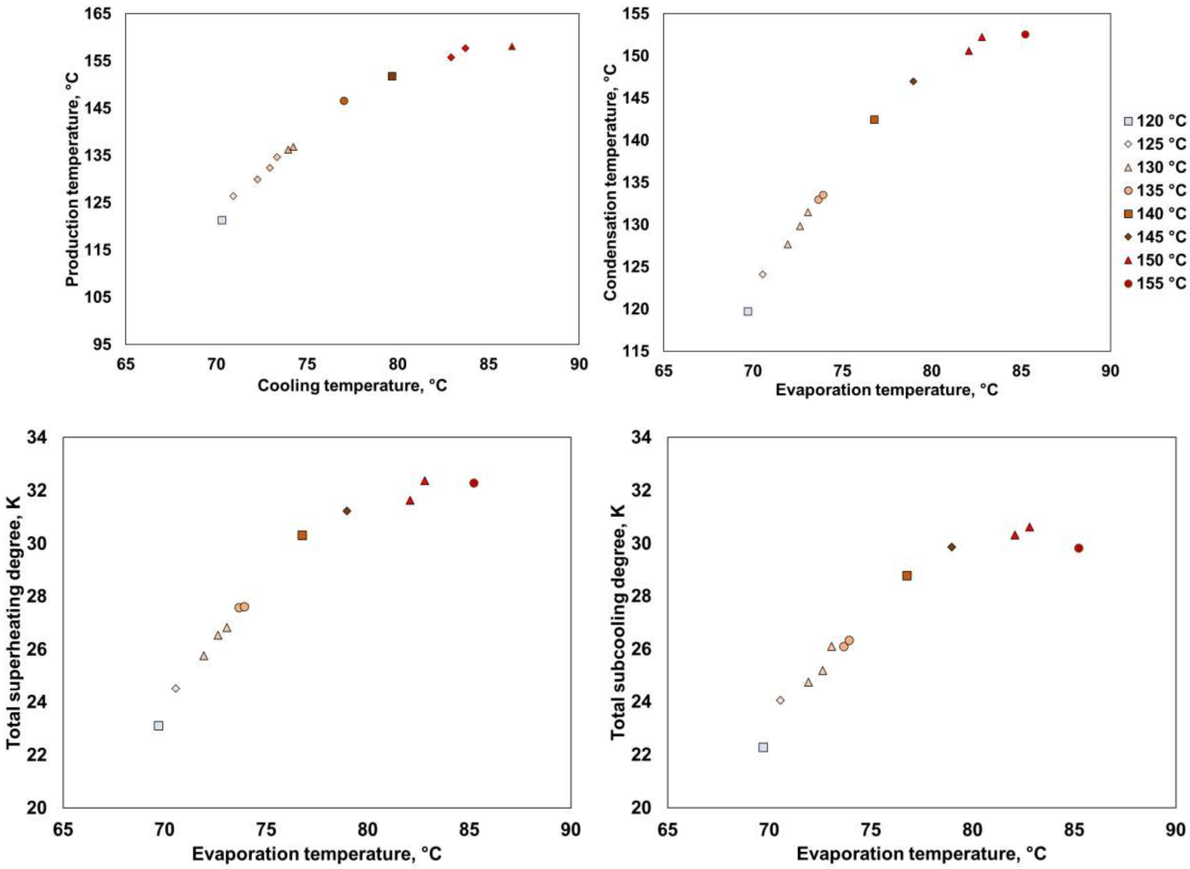

Figure 2: Cooling and production temperatures, condensation temperature, total superheating and subcooling degree versus evaporation temperature

3. RESULTS

3.1. Operational parameters

This section presents experimental measurements and calculations determining the HTHP suitability as renewable heating technology when tested at 40 Hz and high-temperature conditions. The exact condensation temperature can be seen in Figure 2 (top), and the legend must be interpreted as an approximation (±2.5K). The first operational parameter analysed is the pressure ratio, Figure 3. The pressure ratio is the ratio of the discharge and suction pressures measured at the outlet and inlet of the compressor pipeline. Therefore, the final compressor pressure ratio would be higher than the one shown in the following. Attending to the results, it can be seen as the system presented results above 78 °C for increasing the pressure ratio, as it slightly decreased.

The temperature difference between condensation and evaporation varied between 69.7 K and 85.2 K. As the pressure ratio is not remarkable compared to other VCC applications, higher temperature differences were avoided to limit discharge temperature, which two-stage compression or cascade configurations should cover.

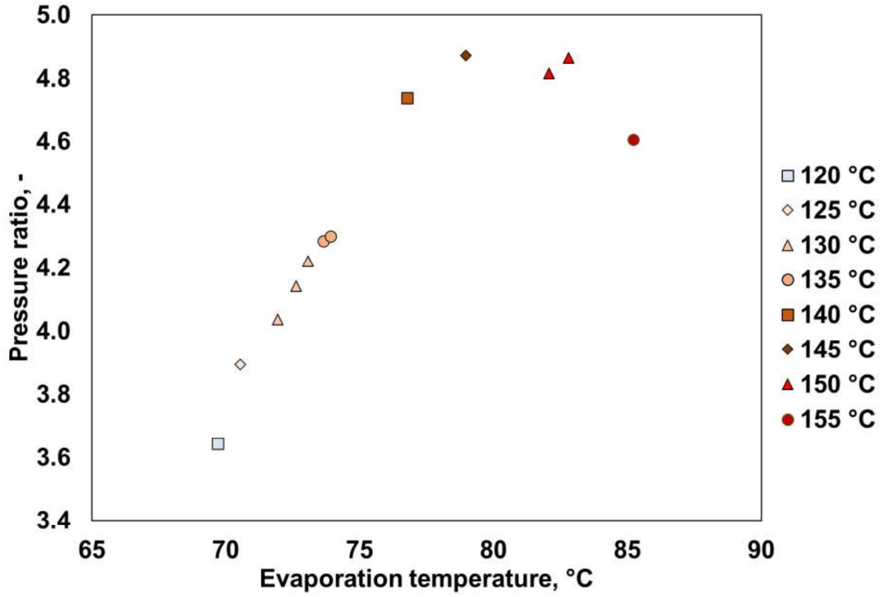

Figure 3: Pressure ratio

Production temperature is directly measured at the condenser outlet on the side of the thermal oil. It simulates the temperature at which an HTF can be heated with an HTHP system. It depends on the condensation temperature and superheating degree, varying between 121.4 °C and 158.1 °C. Moreover, the HTF temperature glides between 8.5 K and 21.8 K, increasing at higher condensation temperatures. Production temperature is limited by desuperheating at the discharge port, pipeline, and heat exchanger design. The discharge temperature is not shown in the article because it is much different from that exits from the compressor discharge port. As a significant difference exists with the ambient temperature, it is significantly affected by the heat losses, and the measured value in the pipeline is diminished.

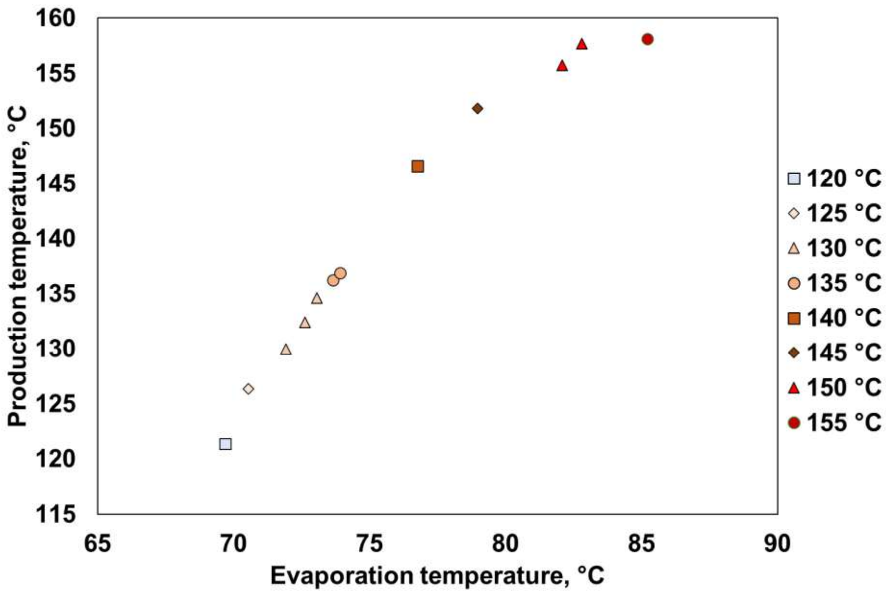

Figure 4: Production temperature

The mass flow rate is directly measured and is affected by compressor suction conditions, pressure drops, compressor operation, and volumetric efficiency. Mass flow rate values vary from 76 g s^{-1} to 110 g s^{-1}. In this case, the frequency was set at 40 Hz, so a higher mass flow rate could be obtained using this compressor. R-1336mzz(Z) suction density is smaller than other refrigerants (18.1 kg m^{-3} to 25.7 kg m^{-3}); therefore, a higher mass flow rate is expected using this installation with other low GWP alternatives.

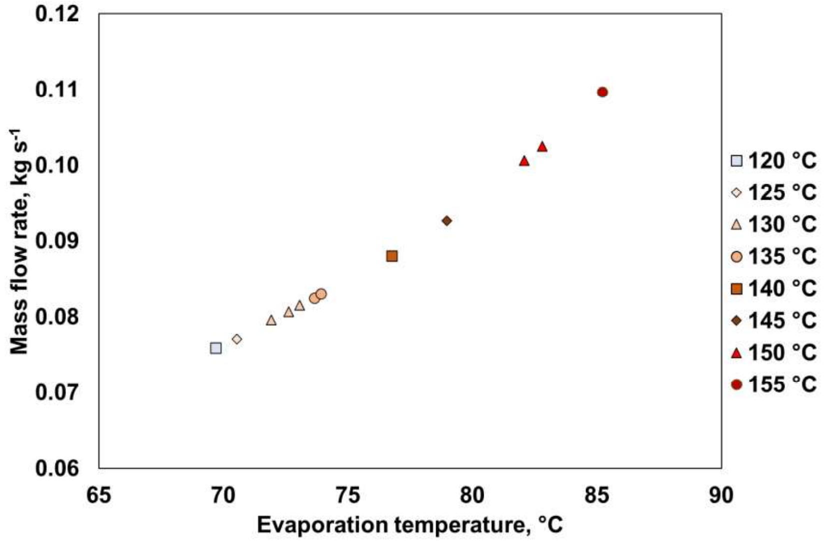

Figure 5: Mass flow rate

3.2. Energy parameters

Once the operational performance of the HTHP prototype has been analysed under high-temperature conditions, the energy performance is discussed in this section. The first parameter analysed is the condenser heating capacity (Figure 6), determined on the refrigerant side as the product of the mass flow rate and the enthalpy difference at the condenser. The condenser heating capacity varies between 9.2 kW and 10.1 kW, being the minimum at an intermediate condition. As observed in the previous section, the mass flow rate decreases at higher evaporation temperatures. However, with a higher condensation temperature set for a higher evaporation temperature, the heating effect (condenser enthalpy difference) decreases (influenced by the decrement in the latent heat aggravated close to the critical point). Therefore, two opposite effects are reflected in the resulting heating capacity.

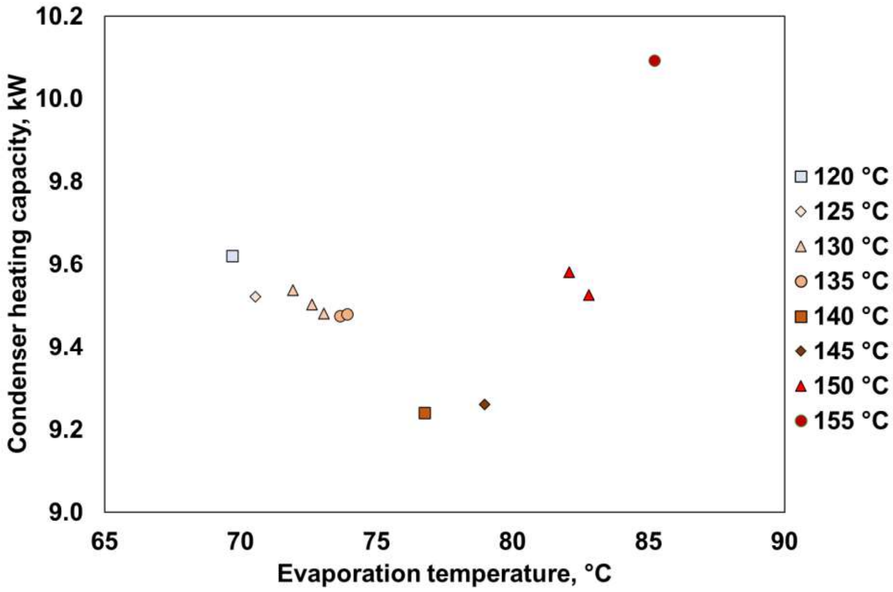

Figure 6: Heating capacity

Finally, the heating coefficient of performance (COP) is presented in Figure 7. The COP is calculated as the ratio of the heating capacity to the measured compressor power consumption. As in standard VCC, it decreases with the increase in pressure ratio. The COP varied from 3.11 to 1.91, being considered adequate for producing economically viable substitutions for boilers and environmentally friendly technology if the electricity is provided at a low carbon emission factor.

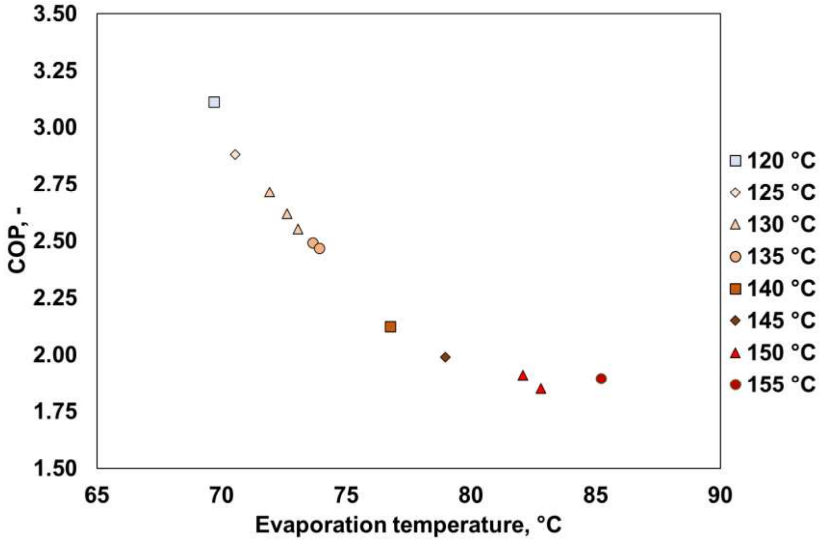

Figure 7: Heating COP

3.3. Comparison with previous results and 50 Hz

The presented results are compared with previous results published by Arpagaus and Bertsch (2019) considering a semi-hermetic alternative compressor, the most comprehensive experimental work published with R-1336mzz(Z) till today. They obtained COP between approximately 1.7 and 4.3, mainly depending on the temperature lift (30 K to 70 K). They have also reached a temperature production of 150 °C, 8 K below results here presented. When they compared R-1336mzz(Z) with other alternatives, this refrigerant presented a slightly lower COP but recognised the potential of reaching higher condensation temperatures. COP values presented in the present work and Arpagaus and Bertsch (2019) are maximised by the LSHX effect, which proved beneficial in previous theoretical and experimental works.

In the following, additional measurements at 50 Hz and lower evaporation and condensation temperature are compared with R-245fa's published results in Mateu-Royo et al. (2019b). Both refrigerants were tested at 50 Hz, but the scroll compressor used with R-1336mzz(Z) was a commercial component, unlike R-245fa, an early prototype (Table 2). The minimum R-245fa evaporation and condensation temperatures were significantly lower than R-1336mzz(Z), and conditions corresponding to moderate HTHP were considered. The pressure ratio tested using R-245fa was also significantly higher than R-1336mzz(Z), and this caused a notably lower COP, affecting viability compared to traditional solutions. R-245fa heating capacity with a similar compression displacement is much lower and confirms it as an unsuitable drop-in replacement if this parameter is considered critical in operation.

Table 2: Comparison of author's experimental campaigns using R-245fa Mateu-Royo et al. (2019b) **and R-1336mzz(Z) at 50 Hz**

Refrigerant	$T_{source,out}$	$T_{sink,out}$	T_{evap}	T_{cond}	PR	$\dot{m}_{ref}$	T_{prod}	$\dot{Q}_{prod}$	COP
	°C	°C	°C	°C	-	g s^{-1}	°C	kW	-
R-1336mzz(Z)	69.4	101.9	65.8	100.7	2.82	85.4	101.9	12.1	4.36
R-1336mzz(Z)	70.5	128.8	71.5	127.1	4.21	96.4	128.8	11.5	2.63
R-245fa	49.0	90.0	38.2	86.7	4.15	47.5	90.0	9.0	2.77
R-245fa	66.3	140.0	64.1	132.3	4.98	100.7	140.0	13.9	1.77

4. CONCLUSIONS

This paper presented one of the first experimental assessments of a high-temperature heat pump prototype (designed for R-245fa) using a scroll compressor and LSHX operating with the low GWP potential refrigerant R-1336mzz(Z). This refrigerant is an alternative to R-245fa operational conditions because it is the only high-temperature synthetic fluid with low GWP and zero ODP. The experimental discussion was focused on high-temperature conditions, for which a 40 Hz frequency was selected for the compressor. Then, tests at 50 Hz were compared to R-245fa.

For the 40 Hz condition, the heating capacity varied between 9.2 and 10.1 kW, and the coefficient of performance was between 1.9 and 3.1. The total superheating degree varied between 23.1 and 32.4 K, provided mainly by the liquid-to-suction heat exchanger, contributing to preventing wet compression. Compared to previous experimental results using R-245fa at 50Hz, R-1336mzz(Z) results in higher COP under comparable operating conditions benefitted by a low-pressure ratio. Attending to the negligible global warming potential of R-1336mzz(Z) and high energy performance, a medium-to-low electricity carbon emission factor would make this solution more environmentally friendly than a natural gas boiler for small-scale heating production.

Future works could focus on alternative R-245fa refrigerants in the form of pure and mixture fluids. The maximum production temperature could be increased and validate the oil degradation. Moreover, limitations related to the compressor discharge temperature and secondary circuits should be resolved with installation modifications.

ACKNOWLEDGEMENTS

This scientific publication is part of the projects UJI-B2018-24 and UJI.>LAB IMPULS/2022/02, funded by Universitat Jaume I. Adrián Mota-Babiloni acknowledges contract IJC2019-038997-I, funded by MCIN/AEI/10.13039/501100011033. Pau Giménez-Prades acknowledges grant CIACIF/2021/182, funded by the Generalitat Valenciana (GV) and the European Social Fund (ESF). Cosmin Mihai Udroiu acknowledges grant PRE2021-097369 funded by MCIN/AEI/10.13039/501100011033 and by "ESF Investing in your future".

NOMENCLATURE

COP	coefficient of performance (-)	*cond*	condensation
evap	evaporation	HCFO	hydrochlorofluoroolefin
HFO	hydrofluoroolefin	HTHP	high-temperature heat pump
HTF	heat transfer fluid	GWP	global warming potential
LSHX	liquid-to-suction heat exchanger	*PR*	pressure ratio (-)
prod	production	*Q*	heat transfer (kW)
m_{ref}	refrigerant mass flow rate (g s^{-1})	ODP	ozone depletion potential
T	temperature (°C)	VCC	vapour compression cycle

REFERENCES

Arpagaus, C., Bertsch, S., 2021. Experimental Comparison of HCFO and HFO R1224yd(Z), R1233zd(E), R1336mzz(Z), and HFC R245fa in a High Temperature Heat Pump up to 150 °C Supply Temperature, in: 18th International Refrigeration and Air Conditioning Conference. Purdue.

Arpagaus, C., Bertsch, S.S., 2019. Experimental results of HFO/HCFO refrigerants in a laboratory scale HTHP with up to 150 °C supply temperature. 2nd Conference on High Temperature Heat Pumps, Copenhagen, Denmark.

Giménez-Prades, P., Navarro-Esbrí, J., Arpagaus, C., Fernández-Moreno, A., Mota-Babiloni, A., 2022. Novel molecules as working fluids for refrigeration, heat pump and organic Rankine cycle systems. Renewable and Sustainable Energy Reviews 167, 112549. https://doi.org/https://doi.org/10.1016/j.rser.2022.112549

Jiang, J., Hu, B., Wang, R.Z., Deng, N., Cao, F., Wang, C.C., 2022. A review and perspective on industry high-temperature heat pumps. Renewable and Sustainable Energy Reviews 161, 112106. https://doi.org/10.1016/J.RSER.2022.112106

Mateu-Royo, C., Navarro-Esbrí, J., Mota-Babiloni, A., Amat-Albuixech, M., Molés, F., 2019a. Thermodynamic analysis of low GWP alternatives to HFC-245fa in high-temperature heat pumps: HCFO-1224yd(Z), HCFO-1233zd(E) and HFO-1336mzz(Z). Appl Therm Eng 152, 762–777. https://doi.org/10.1016/j.applthermaleng.2019.02.047

Mateu-Royo, C., Navarro-Esbrí, J., Mota-Babiloni, A., Molés, F., Amat-Albuixech, M., 2019b. Experimental exergy and energy analysis of a novel high-temperature heat pump with scroll compressor for waste heat recovery. Appl Energy 253, Article 113504. https://doi.org/10.1016/j.apenergy.2019.113504

Obrist, M.D., Kannan, R., McKenna, R., Schmidt, T.J., Kober, T., 2023. High-temperature heat pumps in climate pathways for selected industry sectors in Switzerland. Energy Policy 173, 113383. https://doi.org/https://doi.org/10.1016/j.enpol.2022.113383

Saini, P., Ghasemi, M., Arpagaus, C., Bless, F., Bertsch, S., Zhang, X., 2023. Techno-economic comparative analysis of solar thermal collectors and high-temperature heat pumps for industrial steam generation. Energy Convers Manag 277, 116623. https://doi.org/https://doi.org/10.1016/j.enconman.2022.116623

EFCTC, 2021. Published evidence supports very low yield of TFA from most HFOs and HCFOs Atmospheric breakdown of HFOs and HCFOs containing the CF3CH= moiety. Brussels.